UC Davis
UC Davis Previously Published Works

Title

Comparative transcriptomics and metabolomics reveal specialized metabolite drought stress responses in switchgrass (Panicum virgatum)

Permalink

Journal

ISSN

Authors

Tiedge, Kira
Li, Xingxing
Merrill, Amy T
et al.

Publication Date

DOI

Peer reviewed

Comparative transcriptomics and metabolomics reveal specialized metabolite drought stress responses in switchgrass (*Panicum virgatum*)

Kira Tiedge[1,2] (iD)**, Xingxing Li[3,4]** (iD)**, Amy T. Merrill[5]** (iD)**, Danielle Davisson[1]** (iD)**, Yuxuan Chen[1], Ping Yu[6]** (iD)**, Dean J. Tantillo[5]** (iD)**, Robert L. Last[3,4,7]** (iD) **and Philipp Zerbe[1]** (iD)

[1]Department of Plant Biology, University of California, Davis, Davis, CA 95616, USA; [2]Groningen Institute for Evolutionary Life Sciences, University of Groningen, 9747 AG Groningen, the Netherlands; [3]Department of Biochemistry and Molecular Biology, Michigan State University, East Lansing, MI 48824, USA; [4]DOE Great Lakes Bioenergy Research Center, Michigan State University, East Lansing, MI 48824, USA; [5]Department of Chemistry, University of California, Davis, Davis, CA 95616, USA; [6]NMR Facility, University of California, Davis, Davis, CA 95616, USA; [7]Department Plant Biology, Michigan State University, East Lansing, MI 48824, USA

Author for correspondence:
Philipp Zerbe
Email: pzerbe@ucdavis.edu

Summary

- Switchgrass (*Panicum virgatum*) is a bioenergy model crop valued for its energy efficiency and drought tolerance. The related monocot species rice (*Oryza sativa*) and maize (*Zea mays*) deploy species-specific, specialized metabolites as core stress defenses. By contrast, specialized chemical defenses in switchgrass are largely unknown.
- To investigate specialized metabolic drought responses in switchgrass, we integrated tissue-specific transcriptome and metabolite analyses of the genotypes Alamo and Cave-in-Rock that feature different drought tolerance.
- The more drought-susceptible Cave-in-Rock featured an earlier onset of transcriptomic changes and significantly more differentially expressed genes in response to drought compared to Alamo. Specialized pathways showed moderate differential expression compared to pronounced transcriptomic alterations in carbohydrate and amino acid metabolism. However, diterpenoid-biosynthetic genes showed drought-inducible expression in Alamo roots, contrasting largely unaltered triterpenoid and phenylpropanoid pathways. Metabolomic analyses identified common and genotype-specific flavonoids and terpenoids. Consistent with transcriptomic alterations, several root diterpenoids showed significant drought-induced accumulation, whereas triterpenoid abundance remained predominantly unchanged. Structural analysis verified select drought-responsive diterpenoids as oxygenated furanoditerpenoids.
- Drought-dependent transcriptome and metabolite profiles provide the foundation to understand the molecular mechanisms underlying switchgrass drought responses. Accumulation of specialized root diterpenoids and corresponding pathway transcripts supports a role in drought stress tolerance.

Introduction

Water scarcity exacerbated by climate change threatens biofuel and food crop production across the world (Challinor *et al.*, 2014; W. Kim *et al.*, 2019; Pokhrel *et al.*, 2021). In the United States, about one-third of all counties are currently designated as crop loss disaster areas through drought by the US Department of Agriculture (USDA Farm Service Agency, 2021). Crop production is further impacted by climate-associated increases in pest and pathogen damage (Newbery *et al.*, 2016), calling for new solutions to develop crops that can withstand current and future climate conditions.

The perennial grass switchgrass (*Panicum virgatum*) is a characteristic species of North American tallgrass prairie land and of agroeconomic value as a C$_4$ lignocellulosic feedstock (McLaughlin *et al.*, 1999). A high net-energy yield and environmental resilience make switchgrass economically viable for biofuel production on marginal lands with reduced agricultural inputs. Two major switchgrass ecotypes, northern upland and southern lowland, differ in climatic and geographical adaptation, morphological characteristics and genetic architecture (Lowry *et al.*, 2014; Ayyappan *et al.*, 2017). Upland ecotypes are mostly octoploid ($2n = 8x = 72$), whereas lowland ecotypes are predominantly tetraploid ($2n = 4x = 36$) and feature taller phenotypes with thicker stems and a later flowering time (Casler *et al.*, 2011). The recent development of genome resources for the allotetraploid lowland ecotype Alamo (*c.* 1.23 Gb, NCBI:tx-id38727) (Lovell *et al.*, 2021) now provides the foundation

needed to investigate genetic and biochemical mechanisms underlying switchgrass environmental resilience. Indeed, genomic analysis of 732 switchgrass genotypes across 1800 km latitude range revealed an extensive correlation of genomic architecture to climatic adaptation (Lovell *et al.*, 2021). Comparative morphological and physiological analysis of 49 upland and lowland ecotypes showed significant differences in the drought tolerance of different switchgrass ecotypes (Liu *et al.*, 2015). Large-scale transcriptomic changes were also observed, including a drought-induced downregulation of photosynthetic genes, consistent with physiological responses such as reduced leaf water potential, reduced chlorophyll, and other photosynthetic metabolites (Meyer *et al.*, 2014; Liu *et al.*, 2015; Lovell *et al.*, 2016). Comparative analysis of rhizosheath metabolites further showed an increase in amino acids, carbohydrates and organic acids in response to drought (Liu *et al.*, 2019).

In contrast, knowledge of the contribution of specialized metabolites to switchgrass stress response mechanisms has remained largely unexplored. For example, drought-induced alterations in terpenoid and phenylpropanoid metabolism have been reported (Meyer *et al.*, 2014). In addition, a recent study demonstrated ecotype-specific metabolomes, comprising distinct compositions of specialized steroidal saponins, sesquiterpenoids, diterpenoids, and flavonoids (Li *et al.*, 2022). Our prior work revealed an expansive network of terpenoid-metabolic *terpene synthase* (*TPS*) and *cytochrome P450 monooxygenase* (*P450*) genes in *P. virgatum* var. Alamo, and combined metabolite and transcript profiling illustrated the formation of species-specific diterpenoids and the corresponding biosynthetic genes in switchgrass leaves and roots exposed to ultraviolet (UV) radiation and oxidative stress (Pelot *et al.*, 2018; Muchlinski *et al.*, 2019; Tiedge *et al.*, 2020). Furthermore, emission of volatile monoterpenoids and sesquiterpenoids was observed from switchgrass leaves and roots upon herbivore stress and treatment with defense-related plant hormones (Muchlinski *et al.*, 2019). These collective insights support the importance of terpenoids and other specialized metabolite classes for switchgrass abiotic and biotic stress tolerance. Recent maize (*Zea mays*) and rice (*Oryza sativa*) studies showing induced diterpenoid formation under UV, oxidative and drought stress and decreased abiotic stress tolerance in diterpenoid-deficient maize mutants support a broader role of terpenoids in abiotic stress adaptation in monocot crops (Park *et al.*, 2013; Schmelz *et al.*, 2014; Horie *et al.*, 2015; Vaughan *et al.*, 2015; Ding *et al.*, 2021).

A deeper understanding of the biosynthesis, diversity, and relevance of specialized metabolites for drought responses and more broadly climatic adaptation in perennial biofuel crops can provide resources to improve breeding strategies for developing locally and broadly adapted feedstock systems (Morrow *et al.*, 2014). In this study, we integrated tissue-specific transcriptome and metabolite analyses to investigate specialized metabolism responses to drought in two major switchgrass ecotypes with distinct habitats and contrasting drought tolerance (Liu *et al.*, 2015), namely the lowland Alamo and the upland Cave-in-Rock genotypes.

Materials and Methods

Plant material and treatment

Switchgrass (*P. virgatum* L.), genotypes Alamo AP13 and Cave-in-Rock were kindly provided by Dr Malay Saha (Noble Research Institute, Ardmore, OK, USA). Plants were propagated from tillers to maintain low genetic variation and cultivated in glasshouses to the reproductive stage (R1) under ambient photoperiod and *c.* 27°C : 22°C, day : night temperature prior to drought treatment in a random block design. Following prior drought studies (Liu *et al.*, 2015), drought stress was applied by withholding water consecutively for 4 wk, whereas control plants were watered daily. Volumetric soil water content (SWC) was monitored regularly using a HydroSense II (Campbell Scientific, Logan, UT, USA). Leaf and root tissues of treated and control plants (*n* = 6 per group) were collected before the start of the treatment (week 0), after 2 wk (week 2), and after 4 wk (week 4) at a consistent time and immediately flash-frozen in liquid nitrogen (N_2). To enable comparative data integration, samples for transcriptome and metabolite analyses originated from the same plant tissue samples, which were split for the different analyses.

RNA isolation, transcriptome sequencing, and differential gene expression analysis

Total RNA was extracted from 100 mg of leaves or roots of Alamo and Cave-in-Rock plants (*n* = 6) either drought-stressed or well-watered (control) using a Monarch® Total RNA Miniprep Kit (New England Biolabs, Ipswich, MA, USA) and subsequently treated with DNase I for genomic DNA removal. Following assessment of RNA integrity and quantitation using the Bioanalyzer 2100 RNA Nano 6000 Assay Kit (Agilent Technologies, Santa Clara, CA, USA), four of the six biological replicates with highest RNA quality were selected for sequencing. Preparation of complementary DNA (cDNA) libraries and transcriptome sequencing was performed at Novogene (Novogene Corp. Inc., Sacramento, CA, USA). In brief, following RNA integrity analysis and quantitation, cDNA libraries were generated using a NEBNext® Ultra™ RNA Library Prep Kit (New England Biolabs) and sequenced on an Illumina Novaseq 6000 sequencing platform generating 40–80 million 150 bp paired-end reads per sample. Filtered, high-quality reads were aligned to the reference genome (*P. virgatum* var. Alamo AP13 v.5.1) using Hɪsᴀᴛ2 (D. Kim *et al.*, 2019). Gene functional annotation was based on best matches to databases from Pʜʏᴛᴏᴢᴏᴍᴇ v.13 (phytozome-next.jgi.doe.gov), including Arabidopsis, rice, Gene Ontology (GO), and Panther, as well as in-house protein databases of biochemically verified terpene-metabolic enzymes (Pelot *et al.*, 2018; Murphy & Zerbe, 2020). Differentially expressed genes (DEGs) were identified based on adjusted *P*-value (P_{adj}) < 0.05 and |log$_2$FoldChange (FC)| > 1 as selection criteria. Statistical analyses were conducted in R and also plots and heatmaps were created using the ɢɢᴘʟᴏᴛ2 and ᴘʜᴇᴀᴛᴍᴀᴘ packages in R (cran-project.org, v.3.6.3).

Metabolite extraction

Metabolite analysis followed previously established protocols (Liu *et al.*, 2020). Here, 100 mg tissue were ground to a fine powder in liquid N_2 and metabolites were extracted with 1 ml 80% methanol containing 1 µM telmisartan internal standard by vortexing briefly and incubation for 16 h at 200 rpm and 4°C. Samples were centrifuged for 20 min (4000 **g**, 4°C) to remove solid particles and the supernatants transferred into fresh vials and stored at −80°C prior to liquid chromatography–mass spectrometry (LC–MS) analysis.

UPLC-ESI-QToF-MS analysis

Reversed-phase ultra-performance liquid chromatography–electrospray ionization–quadrupole time-of-flight–mass spectrometry (UPLC–ESI–QToF–MS) analysis was performed in positive and negative mode following a previously established protocol (Li *et al.*, 2022). In brief, metabolite analyses were performed on a Waters Acquity UPLC system equipped with a Waters Xevo G2-XS QToF MS (Waters, Milford, MA, USA). Metabolite separation was conducted on a UPLC BEH C18 column (2.1 mm × 150 mm, 1.7 µm; Waters) using 10 mM ammonium formate (NH_4HCO_2)–water (solvent A) and 100% acetonitrile (solvent B) as mobile phase and the following parameters: flow rate of 0.4 ml min^{-1}; column temperature 40°C; 10 µl injection; method: 0–1 min (99% A : 1% B), 1–15 min linear gradient to 1% A : 99% B, 15–18 min (1% A : 99% B), 18–20 min (99% A : 1% B); QToF parameters: desolvation temperature of 350°C; desolvation gas flow rate at 600 l h^{-1}; capillary voltage of 3 kV; cone voltage of 30 V. Mass spectra were acquired in continuum mode over *m/z* 50–1500 using data-independent acquisition (DIA) or data-dependent MS/MS acquisition (DDA), with collision potential scanned between 20 and 80 V for the higher-energy function of DIA (and 20–60 V for DDA). For DDA mode, the three most abundant molecular ions were automatically selected to pass through the mass filter for fragmentation analysis at each scan. The MS system was calibrated with sodium formate. Leucine enkephalin served as the lock mass compound without but automated mass correction during DIA data acquisition. Quality control (QC) and reference samples were analyzed every 20 injections to evaluate the stability of the LC–MS system.

Data processing and metabolite mining

The obtained DIA MS data were processed using Progenesis QI (v.3.0; Waters) using retention time (RT) alignment, lock mass correction, peak detection, adduct grouping and deconvolution and the following parameters: sensitivity for peak picking: default; minimum chromatographic peak width: 0.15 min; RT range: 0.3–15.5 min. Annotated metabolites were defined by RT and *m/z* information (designated as features). Before downstream statistical analyses, ion abundances of all detected features were normalized to the internal standard telmisartan, based on five biological replicates. The normalized data

(abundance > 300) were used for statistical analysis using MetaboAnalyst 5.0 (Pang *et al.*, 2021). Kyoto Encyclopedia of Genes and Genomes (KEGG), MassBank, PubChem and MetaboLights databases were used to provide feature annotations based on 10 ppm precursor tolerance, 95% isotope similarity and 10 ppm theoretical fragmentation pattern matches with fragment tolerance. In addition, Canopus was used to predict chemical classes of features of interest based on their MS/MS information (Dührkop *et al.*, 2021) with threshold of confidence level 2 (Sumner *et al.*, 2007). DDA analysis was performed for a pooled sample set to generate positive mode MS/MS spectra for the three most abundant parent ions at each MS survey scan (scan time: 0.2 s). The discovery of specialized metabolites (flavonoid glycosides, sesquiterpenoids, diterpenoids, triterpenoids) was achieved by mining the DDA data with focus on the most abundant metabolites.

NMR analysis of terpenoid metabolites

About 200 g fresh root tissues of Cave-in-Rock plants were harvested. Compound purification was performed according to the method described in the Li *et al.* (2022). The differences are the ethyl acetate and hexane phases (in which the diterpenoids were concentrated) were evaporated to dryness using a SpeedVac vacuum concentrator. The residue was re-dissolved in 8 ml of 95% methanol. Supernatants were transferred to LC vials. Purification was carried out as previously described using a C18 HPLC column (100 mm × 4.6 mm × 5 µm). For nuclear magnetic resonance (NMR) analysis, *c.* 0.4–0.8 mg of each high-performance liquid chromatography (HPLC) purified compounds were dissolved in deuterated chloroform ($CDCl_3$; Sigma-Aldrich, St Louis, MO, USA) containing 0.03% (v/v) tetramethylsilane (TMS). NMR one-dimensional (1D) (proton (^1H) and carbon-13 (^{13}C)) and two-dimensional (2D) (heteronuclear single quantum correlation (HSQC), correlation spectroscopy (COSY), heteronuclear multiple-bond correlation (HMBC) and nuclear Overhauser effect spectroscopy (NOESY)) spectra were acquired as previously described (Pelot *et al.*, 2018) on a Bruker Avance III 800 MHz spectrometer (Bruker Corp., Billerica, MA, USA) equipped with a 5 mm CPTCI cryoprobe using Bruker TopSpin 3.6.1 software and analyzed with MestReNova 14.1 software. Chemical shifts were calibrated against known TMS signals.

Results

To investigate metabolic drought responses in switchgrass, we selected the lowland genotype Alamo (AP13) and the upland genotype Cave-in-Rock which were ranked among the most drought-tolerant and drought-susceptible genotypes in a comparative study of 49 switchgrass varieties (Liu *et al.*, 2015). At the beginning of the reproductive stage (R1), plants were exposed to 4 wk of continuous drought treatment, whereby SWC measured as available water capacity (AWC) remained stable at 75% in well-watered control plants and decreased from 75% to 0% in drought-stressed plants (Supporting Information Fig. S1). Leaf and root tissue of both genotypes and treatment groups was

harvested before the treatment (week 0), after 2 wk (week 2) and after 4 wk (week 4), and samples were subject to transcriptomic and metabolomic analyses. Visual inspection of the plants after 2 wk of drought treatment showed no differences between Alamo and Cave-in-Rock and no significant phenotypic drought symptoms. Between 3 and 4 wk of drought treatment Cave-in-Rock plants displayed an increasing wilting phenotype, whereas Alamo plants showed no or only minor wilting throughout the 4-wk drought treatment (Fig. 1).

Alamo and Cave-in-Rock plants show distinct transcriptomic alterations in response to drought

Illumina Novaseq 6000 RNA-sequencing yielded a total of 2.4 billion and 2.7 billion high-quality reads for Alamo and Cave-in-Rock samples, respectively, representing > 97% of the total reads obtained in both datasets. Alignment of the high-quality sequences against the switchgrass Alamo AP13 genome (phytozome-next.jgi.doe.gov/info/Pvirgatum_v5_1) resulted in average mapping rates of 86% for Alamo and 83% for Cave-in-Rock, thus providing a comprehensive transcriptomic dataset for gene discovery and gene expression analyses. Using this dataset, differential gene expression analysis was performed for

control and drought-treated plants of both genotypes. A total of 565 DEGs were identified in roots and 204 DEGs in leaves (DEG threshold: $P_{adj} < 0.05$; $|\log_2 FC| > 1$) of Alamo plants after 4 wk of drought treatment compared to well-watered control plants (Fig. S2). Cave-in-Rock plants showed stronger drought-induced changes with a total of 1198 DEGs in roots and 1120 DEGs in leaves; constituting two- and five-fold more DEGs as compared to Alamo roots and leaves, respectively (Fig. S2). In addition, Cave-in-Rock plants showed an earlier onset of transcriptomic changes compared to Alamo. After 2 wk of watering withdrawal, 2951 and 897 genes were differentially expressed in Cave-in-Rock leaves and roots, respectively, whereas only 19 and 128 genes were differentially expressed in Alamo leaves and roots (Table S1), concurrent with the earlier onset of phenotypic drought symptoms in Cave-in-Rock (Fig. S2). Furthermore, differential gene expression was more pronounced in roots than leaves in both genotypes. Indeed, permutational multivariate analysis of variance (PERMANOVA) illustrated that tissue type (leaves or roots) had the predominant impact on gene expression levels (38.6%, ***, $P < 0.001$), followed by genotype (8%, **, $P < 0.003$) and stress treatment (6%, **, $P < 0.007$) (Table S2).
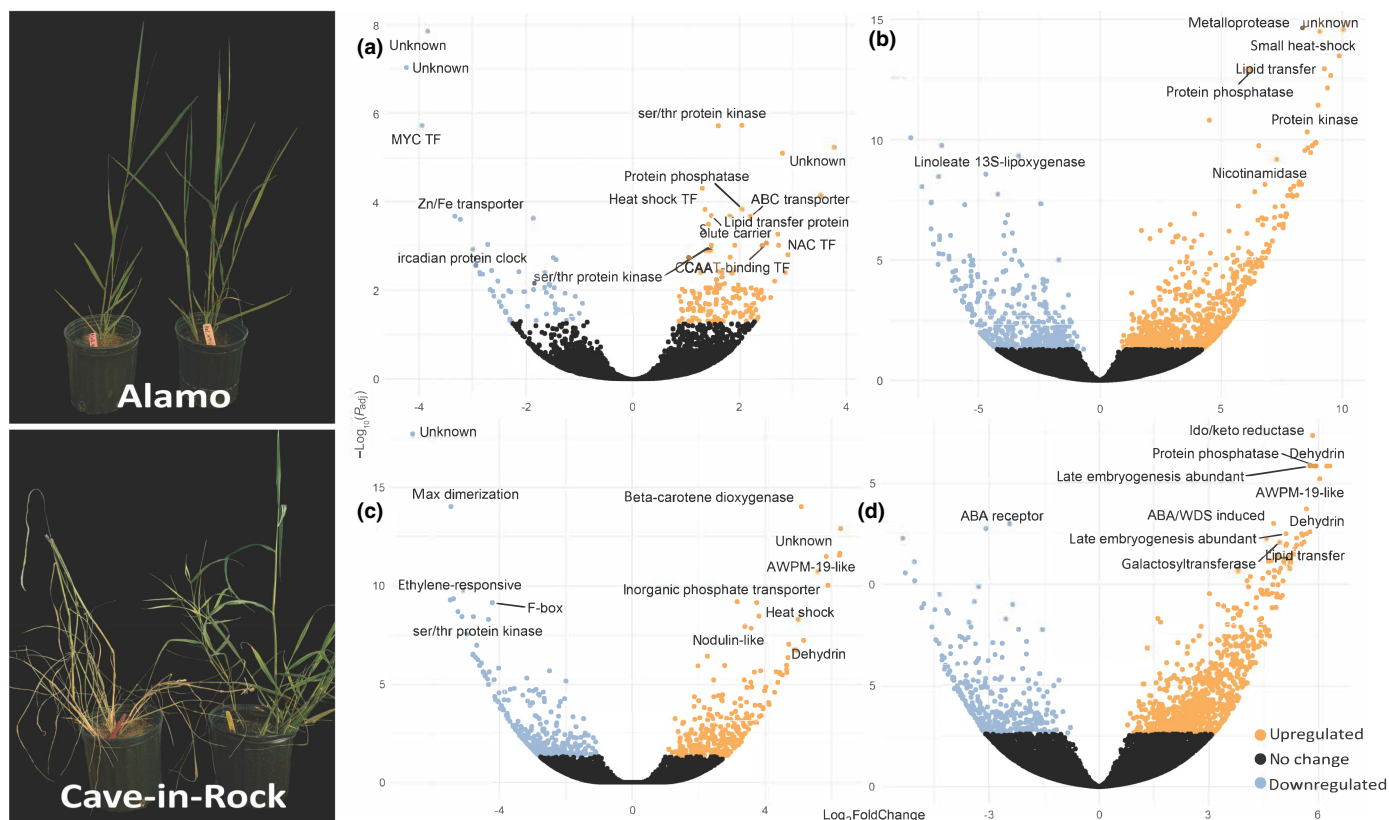

Fig. 1 Left panel: Photographs of switchgrass (*Panicum virgatum*) Alamo and Cave-in-Rock plants after 4 wk of drought treatment (+d) or normal watering (−d). Right panels: Volcano plots of differentially expressed genes identified after 4 wk of drought in (a) Alamo leaves, (b) Cave-in-Rock leaves, (c) Alamo roots and (d) Cave-in-Rock roots. Differential expression was performed using the DESeq2 R package. Resulting *P*-values were adjusted for controlling the false discovery rate (FDR). Differential expression of genes with an adjusted *P*-value (P_{adj}) < 0.05 and a log$_2$FoldChange > 1 was assigned as being significantly different.

Major transcriptomic changes include genes of known drought response mechanisms and core general metabolic processes

Consistent with the differences in the number and onset of DEGs between Alamo and Cave-in-Rock, the identified genes showing the most significant differential expression differed between the two genotypes and tissues (Fig. 1). Only two genes, a putative circadian clock protein (*Pavir.9NG553200*) and a predicted lipid transfer protein (*Pavir.5NG603383*) were differentially expressed in all genotypes and tissues (Fig. S2). The genotype- or tissue-specific DEGs included numerous so far uncharacterized genes as well as genes involved in known drought response mechanisms. For example, in roots of both genotypes *dehydrin* (log$_2$FC Alamo = 5.2, CiR = 6.24) and other *Late Embryogenesis Abundant* (*LEA*) genes (log$_2$FC Alamo = 4.34, CiR = 5.78), as well as several *AWPM19-like* plasma-membrane-associated abscisic acid (ABA) influx transporters implicated with drought tolerance (log$_2$FC Alamo = 6.25, CiR = 6.04) were highly upregulated (Fig. 1; Table S1). Notably, among the 11 *AWPM19-like* genes, Alamo and Cave-in-Rock featured distinct genes (*Pavir.2NG274300* in Alamo vs *Pavir.9NG018700* in Cave-in-Rock) as the most differentially expressed *AWPM19-like* genes. The increased expression of known drought-associated genes supports the drought response in both genotypes, despite the visual lack of a wilting phenotype in Alamo plants. Along the lack of a wilting phenotype in Alamo plants, no genes associated with cell death and necrosis processes such as caspases and proteases were present among the differentially upregulated genes (i.e. featured an P_{adj} > 0.05 with a |log$_2$FC| < 1), supporting that the observed expression patterns represent a drought response rather than being associated with drought-related plant death.

Next, we investigated the impact of drought on core metabolic pathways independent of known drought response processes. Among 26 GO terms significantly enriched in all samples combined most encoded for biological processes or molecular functions (Fig. S3). In Alamo leaves DNA-binding and electron carrier processes were most significantly enriched, whereas carbohydrate metabolism was predominant in roots. Interestingly, Cave-in-Rock roots featured highly enriched abiotic stress response processes rather than carbohydrate metabolism under drought stress, whereas leaves showed patterns similar to Alamo with DNA-binding and hydrolase activities being differentially expressed (Fig. S3). Additional pathway enrichment analyses using KEGG terms confirmed a substantially higher number of metabolic pathways enriched in Cave-in-Rock as compared to Alamo, with more genes underlying the enriched pathways on average (Figs 2, S4). Plant signal transduction process ranked among the most significantly enriched in Alamo and Cave-in-Rock leaves, especially in response to drought stress. By contrast,
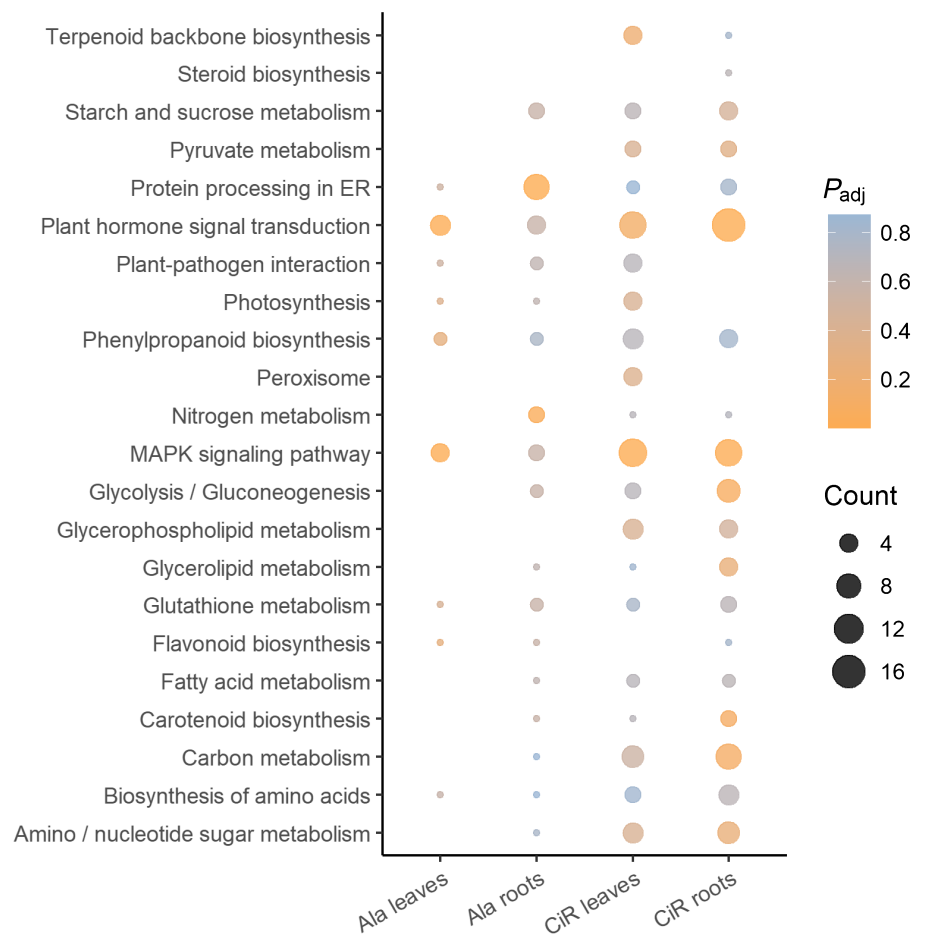

Fig. 2 Kyoto Encyclopedia of Genes and Genomes (KEGG) pathway enrichment analysis of differentially expressed genes in switchgrass (*Panicum virgatum*). Circle color denotes the adjusted *P*-value (P_{adj}), circle size is proportional to the number of genes involved in the enrichment of the pathway (Count). The CLUSTERPROFILER R package was used to test the statistical enrichment of differentially expressed genes in KEGG pathways where genes with an P_{adj} < 0.05 were considered significantly enriched.

endoplasmic reticulum protein processing and nitrogen metabolism were most significantly altered in Alamo and, to lesser degree, in Cave-in-Rock roots (Fig. 2). Albeit at lower levels, pathway enrichment was also observed for general and specialized metabolism, including carbon and amino acid metabolism, as well as carotenoid, steroid, and phenylpropanoid biosynthesis (Fig. 2; Table S3).

Switchgrass features tissue-, genotype- and drought-specific alterations in terpenoid and phenylpropanoid pathways

The enrichment of terpenoid and phenylpropanoid metabolism is consistent with prior studies illustrating ecotype-specific profiles of steroidal saponins and flavonoids (Li *et al.*, 2022), and the upregulation, albeit at moderate levels, of switchgrass terpenoid- and phenylpropanoid-metabolic pathways in response to drought, UV irradiation and oxidative stress (Meyer *et al.*, 2014; Pelot *et al.*, 2018; Muchlinski *et al.*, 2019; Tiedge *et al.*, 2020). To investigate in more detail the impact of drought on switchgrass specialized metabolism, we compared the transcript abundance of key genes of the terpenoid and phenylpropanoid scaffold-forming pathways in both genotypes. Due to the lack of a Cave-in-Rock genome, gene annotations are based on homology searches against the switchgrass Alamo AP13 genome (phytozome-next.jgi.doe.gov/info/Pvirgatum_v5_1). Interestingly, the focal genes showed similar tissue-specific expression profiles in Alamo and Cave-in-Rock and no substantial drought-induced gene expression changes were observed (Fig. 3). For example, of the four annotated *1-deoxyxylulose 5-phosphate synthase* (*DXS*) genes of the methylerythritol phosphate (MEP) pathway, two homologs, *Pavir.3KG128241* and *Pavir.3NG140939*, were abundant in leaves but *c.* 10–60-fold less in roots of both Alamo and Cave-in-Rock (Fig. 3a). Likewise, the predicted squalene synthase, *Pavir.4NG340500*, displayed high abundance in leaves and low gene expression in roots. However, select genes showed genotype-specific differences in their expression patterns. This included the predicted *geranylgeranyl pyrophosphate synthase* (*GGPPS*), *Pavir.6Ng089000*, that was expressed in Alamo but not Cave-in-Rock roots (Fig. 3a). A similar trend of gene expression was observed for core genes of phenylpropanoid metabolism with several annotated *phenylalanine ammonia lyase* (*PAL*), *cinnamate-4-hydroxylase* (*C4H*), and *4-coumaroyl-CoA ligase* (*4CL*) genes showing higher expression in roots as compared to leaves in both Alamo and Cave-in-Rock (Fig. 3b).

Contrasting the largely unaltered and comparable expression of the highly conserved upstream pathway genes, both Alamo and Cave-in-Rock plants featured distinct gene expression profiles for downstream pathway branches that generate species-specific, functionalized metabolites. Following the recent discovery of specialized triterpenoid and steroid saponins in switchgrass (Li *et al.*, 2022), identification and gene expression analysis of predicted *cycloartenol synthases* (*CAS*), *lanosterol synthases* (*LAS*), *β-amyrin synthases* (*BAS*), as well as members of the *CYP71A*, *CYP90B* and *CYP94D* cytochrome P450 families and *sterol 3-β-glucosyltransferases* with known functions in triterpenoid

metabolism revealed distinct expression patterns across tissue type and genotype (Fig. 4). For example, hierarchical gene cluster analysis illustrated predicted *triterpenoid synthase* (*TTS*) genes and a putative *CYP72A* gene with similar inducible expression patterns in Alamo leaves after 2 and 4 wk of drought (Table S4). Likewise, in Alamo roots a different group of *TTS*, *sterol 3-β-glucosyltransferase*, and putative *CYP72A*, *CYP94D* and *CYP90B* genes, known to function in the biosynthesis of triterpenoid saponins such as diosgenin (Ciura *et al.*, 2017), displayed common inducible expression patterns after 4 wk of drought (Fig. 4, upper panel). By contrast, co-expression patterns of triterpenoid-biosynthetic genes were not detectable in Cave-in-Rock (Fig. 4, lower panel).

Our prior research identified expansive, species-specific diterpene synthase (diTPS) and P450 families in switchgrass that form complex metabolic networks toward a range of labdane-related diterpenoids, including *syn*-pimarane and furanoditerpenoid compounds that occur, perhaps uniquely, in switchgrass (Fig. S5) (Pelot *et al.*, 2018; Muchlinski *et al.*, 2021). This pathway knowledge enabled a detailed analysis of transcriptomic alterations related to diterpenoid metabolism. Contrasting the largely similar expression patterns of MEP and mevalonate (MVA) pathway genes (Fig. 3a), hierarchical gene cluster analysis revealed distinct *diTPS* and *P450* gene expression between Alamo and Cave-in-Rock (Fig. 5). In Alamo roots, the *cis-trans-clerodienyl pyrophosphate (CLPP) synthase PvCPS1* and the *P450* genes, *CYP71Z25*, *CYP71Z26*, and *CYP71Z28* shown to form furanoditerpenoids (Muchlinski *et al.*, 2021), showed patterns of co-expression at 2 and 4 wk of drought. Similarly, the predicted *syn-CPP synthases*, *PvCPS9* and *PvCPS10*, as well as two class I diTPS, *PvKSL4* and *PvKSL5*, shown to form *syn*-pimaradiene compounds (Pelot *et al.*, 2018), co-expressed in roots, albeit without significant drought-inducible transcript changes. In Cave-in-Rock, *diTPS* and *P450* genes were expressed mostly in the well-watered plants and water deficiency did not elicit significant transcript accumulation. Also, contrasting roots, no drought-elicited changes in the expression of diterpenoid pathway genes was detectable in leaves of either ecotype.

Switchgrass leaves and roots show drought-inducible metabolite alterations

To complement transcriptomic studies leaf and root metabolomes of Alamo and Cave-in-Rock plants under drought-stressed and well-watered conditions were examined using untargeted liquid chromatography–quadrupole time-of-flight–mass spectrometry (LC–QToF–MS) analysis. Using accurate mass, RT, and fragmentation patterns, we identified 5181 and 3234 metabolite features in positive and negative ion mode, respectively. To compare metabolite profiles across tissues, genotypes, and treatments, after filtering for ion-abundance (see the Materials and Methods section for details) 2519 positive mode mass features (identified as RT : *m*/*z* ratio pairs) were selected for downstream statistical analysis (Table S5).

Aligned with the transcriptomic changes, biostatistical analysis of the untargeted metabolomic data via PERMANOVA showed
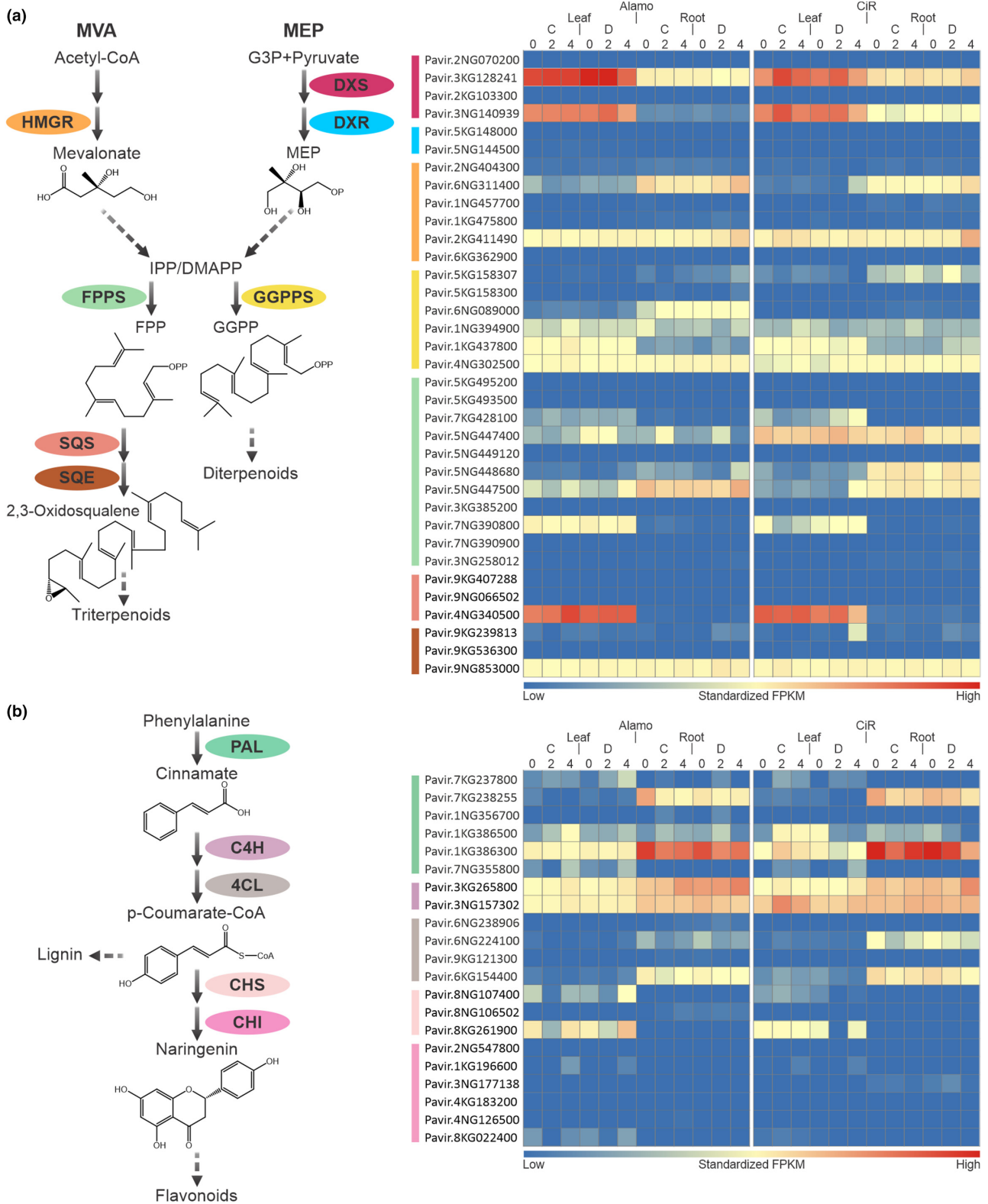
Fig. 3 Plot of normalized gene expression profiles of genes with predicted functions in (a) terpenoid backbone biosynthesis and (b) flavonoid backbone biosynthesis after 0, 2 or 4 wk in drought-treated (D) or well-watered control (C) switchgrass (*Panicum virgatum*) Alamo and Cave-in-Rock (CiR) plants. Gene expression data are based on four biological replicates and gene functional annotations are based on best matches in Bʟᴀsᴛ searches against public and in-house protein databases. Gene IDs are derived from the *P. virgatum* genome v.5.1 (phytozome-next.jgi.doe.gov/info/Pvirgatum_v5_1). DXS, 1-deoxyxylulose 5-phosphate synthase; DXR, 1-deoxyxylulose 5-phosphate reductase; HMGR, HMG-CoA reductase; FPPS, farnesyl pyrophosphate synthase; GGPPS, geranylgeranyl pyrophosphate synthase; SQS, squalene synthase; SQE, squalene epoxidase; PAL, phenylalanine ammonia lyase; C4H, cinnamate-4-hydroxylase; 4CL, 4-coumaroyl-CoA ligase; CHS, chalcone synthase; CHI, chalcone isomerase.
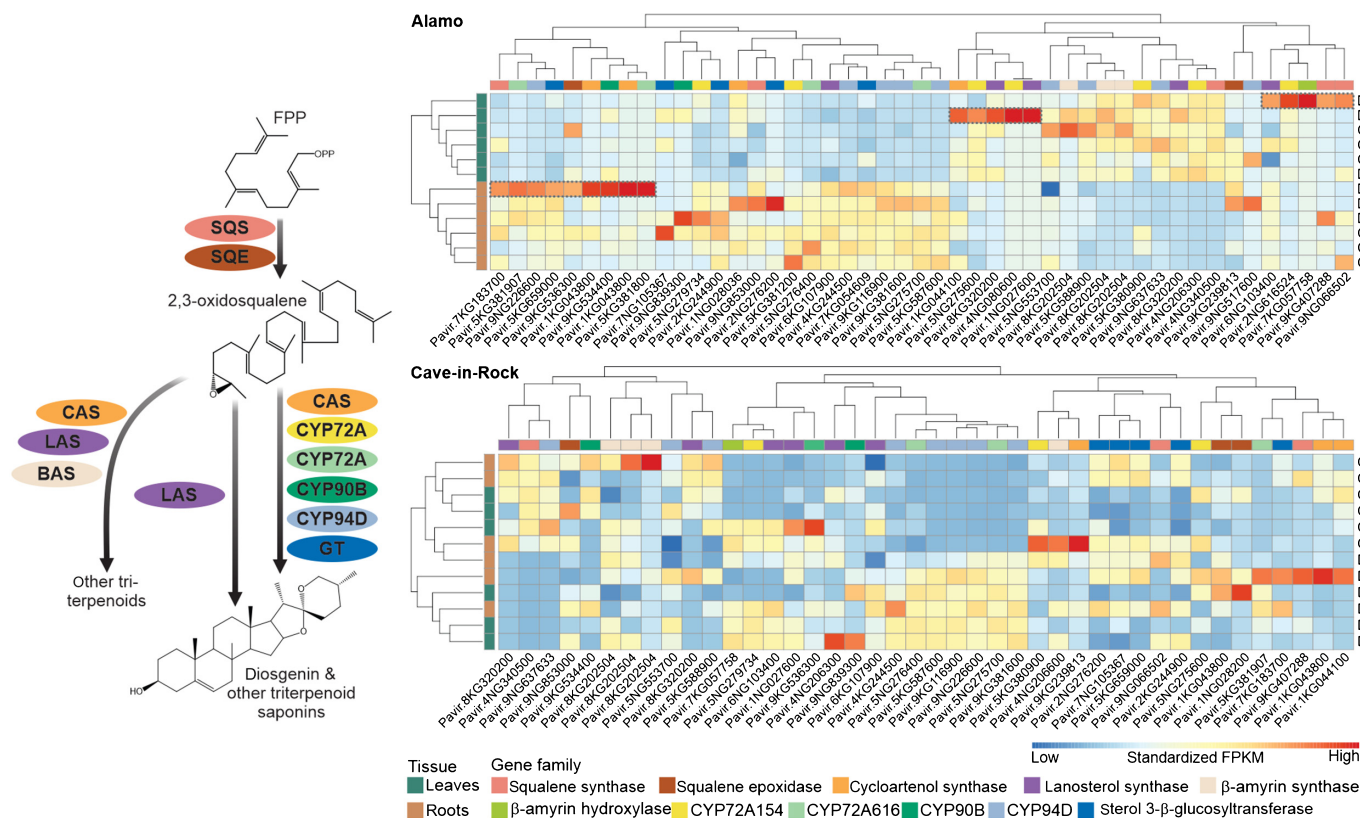
Fig. 4 Hierarchical cluster analysis of select genes with predicted functions in triterpenoid biosynthesis in switchgrass (*Panicum virgatum*) Alamo and Cave-in-Rock plants. Gene functional annotations are based on best matches in BLAST searches against in-house protein databases of known triterpenoid-metabolic genes. Gene IDs are derived from the *P. virgatum* genome v.5.1 (phytozome-next.jgi.doe.gov/info/Pvirgatum_v5_1). Gene expression data are based on four biological replicates. Dashed boxes highlight genes with relevant co-expression patterns. Right side: C0L, C2L, C4L: leaves of well-watered control plants after 0, 2 and 4 wk of treatment; C0R, C2R, C4R: roots of well-watered control plants; D0L, D2L, D4L: leaves of drought-stressed plants; D0R, D2R, D4R: roots of drought-stressed plants.

that tissue type had the highest impact on metabolite composition (72.4%, ***, $P < 0.001$), followed by difference in genotype (2.8%, *, $P < 0.028$) and drought-treatment vs control (0.6%, $P < 0.332$) (Table S2). Hence, we further analyzed the metabolite profiles independently within each tissue type. Despite the relatively lower impact of drought treatment on metabolic alterations, under a multivariate dimension-reduction based on genotype metabolite features clustered together before water deprivation (week 0), but separated in leaves and, to a lesser extent, in roots after 4 wk of drought treatment (Fig. 6). This shift in metabolite composition was driven by several major features (Fig. 7). In leaves, most compounds showing accumulation differences in control and drought-stressed plants were classified as phospholipids based on database searches for each feature. These compounds increased in abundance in Alamo during drought treatment, whereas a decrease was observed in Cave-in-Rock (Fig. 7). In addition to predicted phospholipids, a few features were enriched in Alamo leaves under drought stress, whereas many unidentified compounds were enriched in drought-treated Cave-in-Rock leaves (Table S2). In contrast, several compounds identified as diterpenoids and triterpenoids by comparison of RT and fragmentation patterns to previously identified compounds (Muchlinski *et al.*, 2021; Li *et al.*, 2022)

accumulated in roots of both Alamo and Cave-in-Rock plants under drought stress, with a stronger increase in Alamo (Fig. 7). Other root metabolites that accumulated differentially under drought conditions either did not score significant database matches or could only be assigned to the general classes of carbohydrates, acids, or alcohols (Fig. 7). Among the few features that were generally enriched in both leaves and roots and in both ecotypes under water deficient conditions was also ABA, which was increased by *c.* 40–300-fold under drought (Fig. 8a; Table S6, ABA: 6.08_247.1244 *m/z*).

Drought induces the accumulation of specialized furanoditerpenoids in switchgrass roots

Considering that predicted specialized steroidal and triterpenoid saponins and diterpenoids contribute substantially to the metabolic differences between Alamo and Cave-in-Rock roots, we examined these compounds in more detail in leaf and root extracts after 4 wk of drought where the physiological stress symptoms were most pronounced. Several predicted flavonoid glycosides were identified in leaves of Alamo and Cave-in-Rock plants but were absent in root tissue. However, these compounds showed no or only minimal patterns of drought-elicited
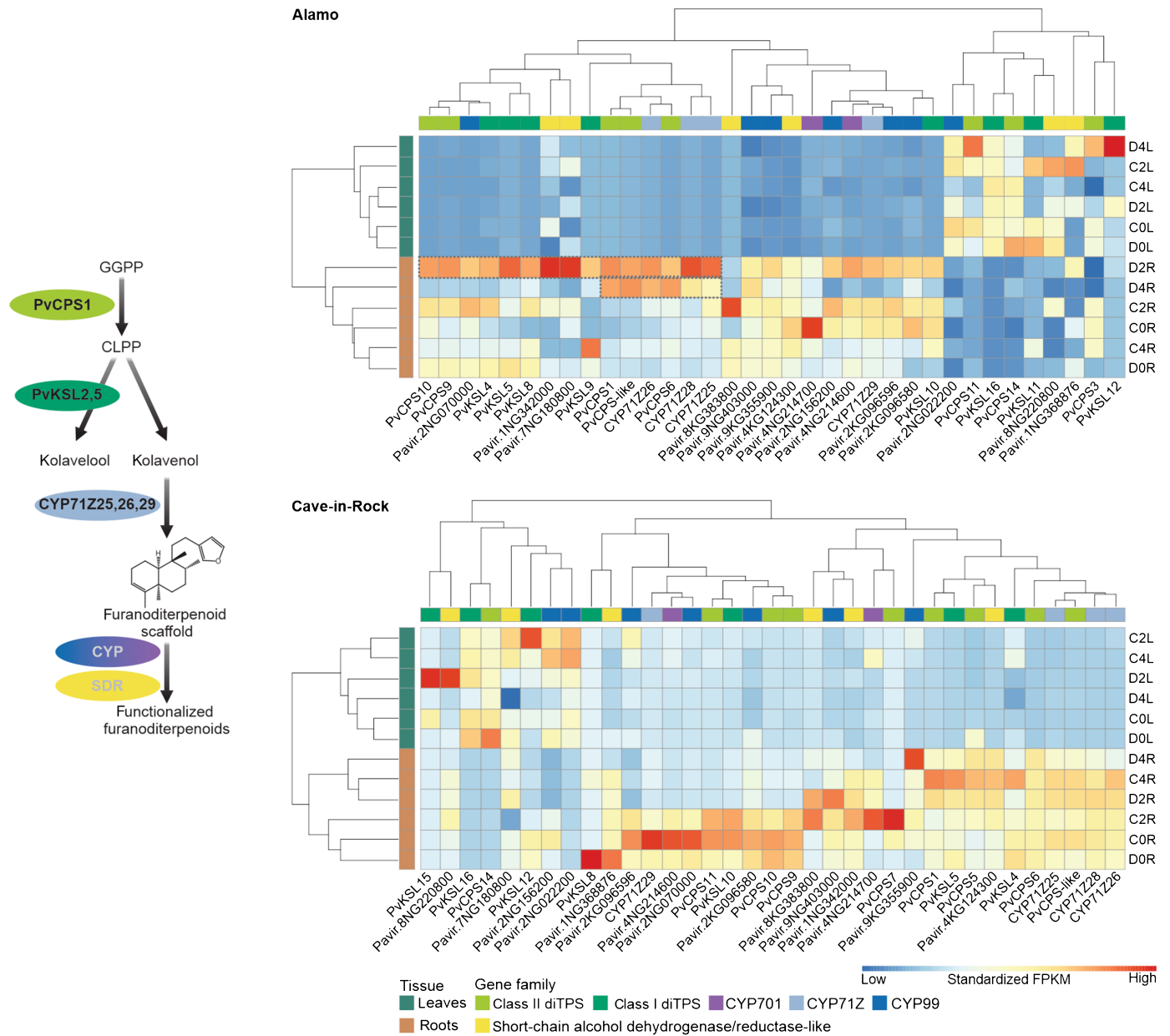
Fig. 5 Hierarchical cluster analysis of select genes with known or predicted functions in diterpenoid biosynthesis in switchgrass (*Panicum virgatum*) Alamo and Cave-in-Rock plants. Gene functional annotations are based on previous biochemical enzyme characterizations or best matches in Bʟᴀsᴛ searches against in-house protein databases of known diterpenoid-metabolic genes. Gene IDs are derived from the *P. virgatum* genome v.5.1 (phytozome-next.jgi. doe.gov/info/Pvirgatum_v5_1). Gene expression data are based on four biological replicates. Dashed boxes highlight genes with relevant co-expression patterns. Solid and dashed arrows indicate characterized and predicted pathway steps, respectively. C0L, C2L, C4L: leaves of well-watered control plants after 0, 2 and 4 wk of treatment; C0R, C2R, C4R: roots of well-watered control plants; D0L, D2L, D4L: leaves of drought-stressed plants; D0R, D2R, D4R: roots of drought-stressed plants.

accumulation (Fig. 8a). In addition, a range of distinct terpenoid metabolites was identified. Among these metabolites, the largest group represented recently identified steroidal or triterpenoid saponins (Li *et al.*, 2022), showing distinct profiles across tissues and genotypes. Triterpenoid saponins occurred predominantly in leaves of both Alamo and Cave-in-Rock plants, whereas the larger group of steroidal saponins were present in leaves and/or roots and occurred predominantly in either Alamo or Cave-in-Rock plants. Despite the overall abundance of these saponins, the vast

majority of the annotated metabolites were not significantly enriched upon drought stress ($P \leq 0.05$; Table S6). In addition to the larger group of triterpenoids, 11 compounds predicted as specialized diterpenoids were identified, the majority of which occurred predominantly in Alamo roots and were absent or abundant at only low levels in Cave-in-Rock (Fig. 8a). Notably, two pairs of predictably isomeric diterpenoids were detected in Alamo and Cave-in-Rock that showed substantial accumulation mostly in drought-stressed roots. One metabolite pair at RTs of
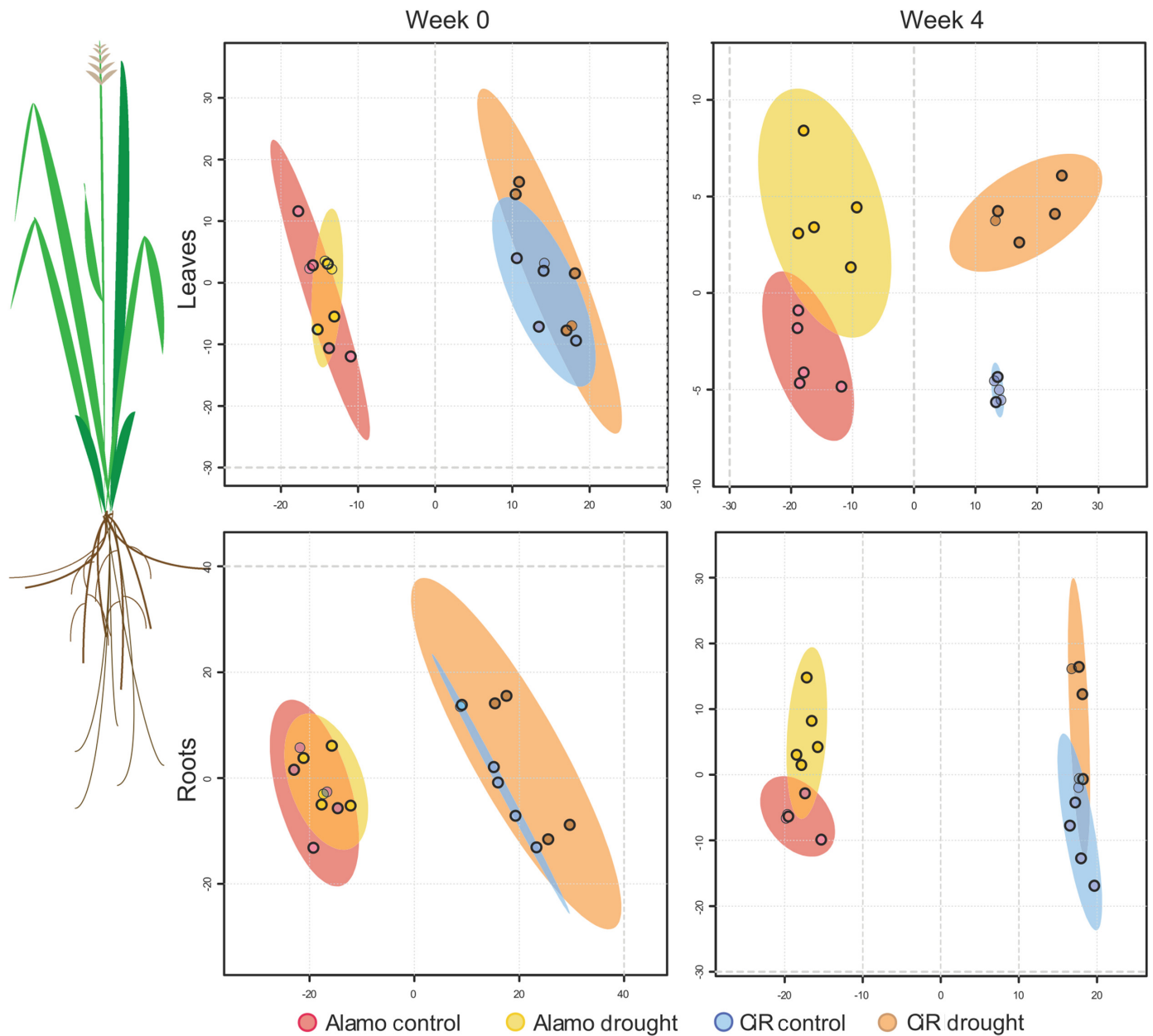
Fig. 6 Partial least-squares discriminant analysis (PLS-DA) plots of liquid chromatography–mass spectrometry (LC–MS) positive mode metabolome divergence based on five biological replicates. *x*-axis, principal component 1; *y*-axis, principal component 2.

9.06 min and 9.26 min featured a dominant precursor mass ion of *m/z* 317 $[M + H]^+$ and one compound pair at RTs of 11.50 min and 11.72 min featured a dominant ion of *m/z* 317 $[M + H]^+$. Together with the presence of additional mass ions of *m/z* 257, *m/z* 189, *m/z* 177 or *m/z* 135, these fragmentation patterns suggested that these compounds represent labdane-related diterpenoids carrying one or more oxygenation functions (Fig. S4). To elucidate the precise structure of these diterpenoids, metabolites were extracted from mature Cave-in-Rock roots and purified via liquid–liquid phase partitioning followed by HPLC. Purified samples (0.4–0.8 mg for each compound) of both *m/z* 301 isomers and both *m/z* 317 diterpenoid isomers were used for 1D (^{1}H and ^{13}C) and 2D (HSQC, COSY, HMBC and NOESY)

NMR analyses. Collectively, the generated data identified the *m/z* 301 diterpenoids as 15,16-epoxy-2-oxo-5α8α-cleroda-3,13 (16),l4-triene and its C19 enantiomer, while the earlier eluting diterpenoid *m/z* 317 was identified as 2-oxo-5α8α-cleroda-3,13-dien-16,l5-olide, together designated as panicoloid A, panicoloid B, and panicoloid C respectively (Figs 8b, S6). Insufficient abundance and purity of the later eluting *m/z* 317 diterpenoid isomer prevented structural analysis of this metabolite. Based on the similar mass fragmentation pattern and RT compared to the other *m/z* 317 isomer (Fig. S4), it is plausible that this compound represents its enantiomeric isomer and is tentatively named panicoloid D. The identified diterpenoids represent derivatives of previously identified switchgrass furanoditerpenoids that feature
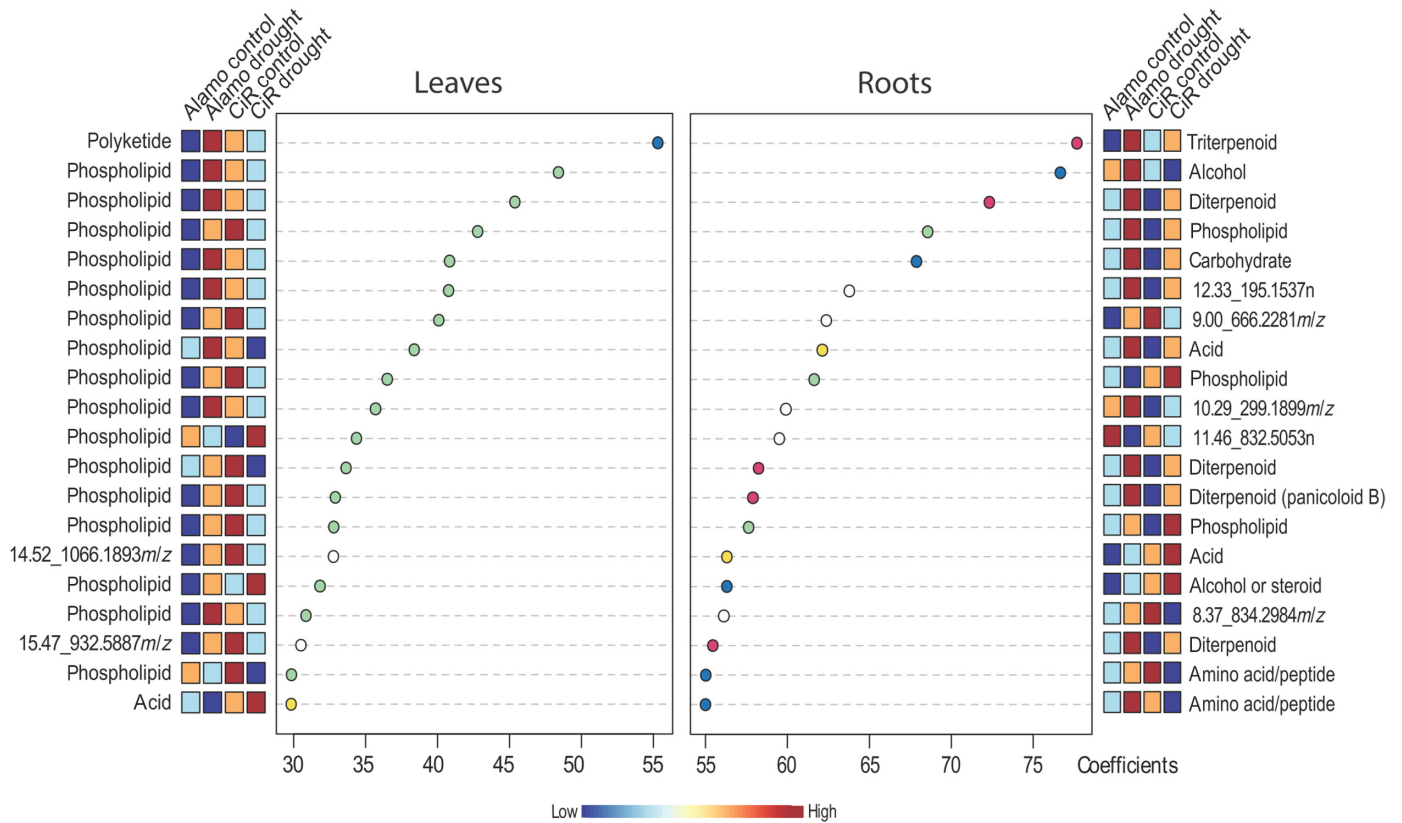
Fig. 7 Scree plot of metabolite features obtained via liquid chromatography–mass spectrometry (LC–MS) positive mode analysis that show the most significant contribution to changes in metabolite profiles in response to drought stress in switchgrass (*Panicum virgatum*) plants. A higher coefficient (*x*-axis) denotes a higher importance for this feature in the partial least-squares discriminant analysis (PLS-DA) shown in Fig. 6. Boxes display the relative abundance of a feature among the different groups as based on five biological replicates. Metabolite annotations are based on matching *m/z* ratios, retention time and fragmentation patterns against online databases.

additional carbonyl functions at C2 and/or C14 and are collectively named here as the group of panicoloids (Fig. S4).

Discussion

Knowledge of the gene-to-metabolite relationships underlying specialized metabolic pathways that contribute to plant stress resilience can enable new crop optimization strategies for addressing exacerbating environmental pressures and associated harvest loss (Savary *et al.*, 2019). Extensive studies in major food and bioenergy crops such as rice, maize, and sorghum (*Sorghum bicolor*) have demonstrated that species-specific blends of specialized terpenoids, phenylpropanoids, oxylipins, and benzoxazinoids mediate complex responses to biotic and abiotic perturbations (Schmelz *et al.*, 2014; Murphy & Zerbe, 2020). By contrast, knowledge of the diversity of specialized metabolites in the perennial bioenergy crop switchgrass and its relevance for drought adaptation in different switchgrass genotypes is incomplete. Combined transcriptome and metabolome analysis of the lowland ecotype Alamo shown to be drought-tolerant and the upland ecotype Cave-in-Rock with low drought tolerance (Liu *et al.*, 2015) revealed common and distinct metabolic alterations and identified specialized diterpenoid metabolites with possible functions in switchgrass drought adaptation.

Consistent with prior studies showing that upland and lowland switchgrass ecotypes have different transcriptomic and metabolite profiles under optimal conditions (Ayyappan *et al.*, 2017; Li *et al.*, 2022), this study demonstrates that metabolic alterations in Alamo and Cave-in-Rock are predominantly driven by differences in tissue type and genotype, thus reflecting the different habitat range and climatic adaptation of switchgrass ecotypes. A stronger wilting phenotype after 4 wk of drought treatment, along with more than twice as many DEGs illustrate more pronounced drought-induced metabolic changes in Cave-in-Rock, consistent with prior studies identifying Cave-in-Rock as particularly drought-susceptible among switchgrass varieties (Liu *et al.*, 2015). Presence of known drought-response genes among the most DEGs in Alamo and/or Cave-in-Rock supported substantial drought responses in both genotypes during drought treatment, despite the lack of significant phenotypic changes in Alamo. Known drought-associated genes included *LEA* genes, including dehydrin shown to impact drought tolerance in Arabidopsis and cotton (*Gossypium spec.*) (Olvera-Carrillo *et al.*, 2010; Magwanga *et al.*, 2018), a NAC transcription factor (*Pavir.8KG003520*) shown to contribute to drought tolerance in a recent switchgrass genome-wide association study (GWAS) (Lovell *et al.*, 2021), and AWPM-19-like ABA influx transporters (Yao *et al.*, 2018), Differential expression of several AWPM-19-
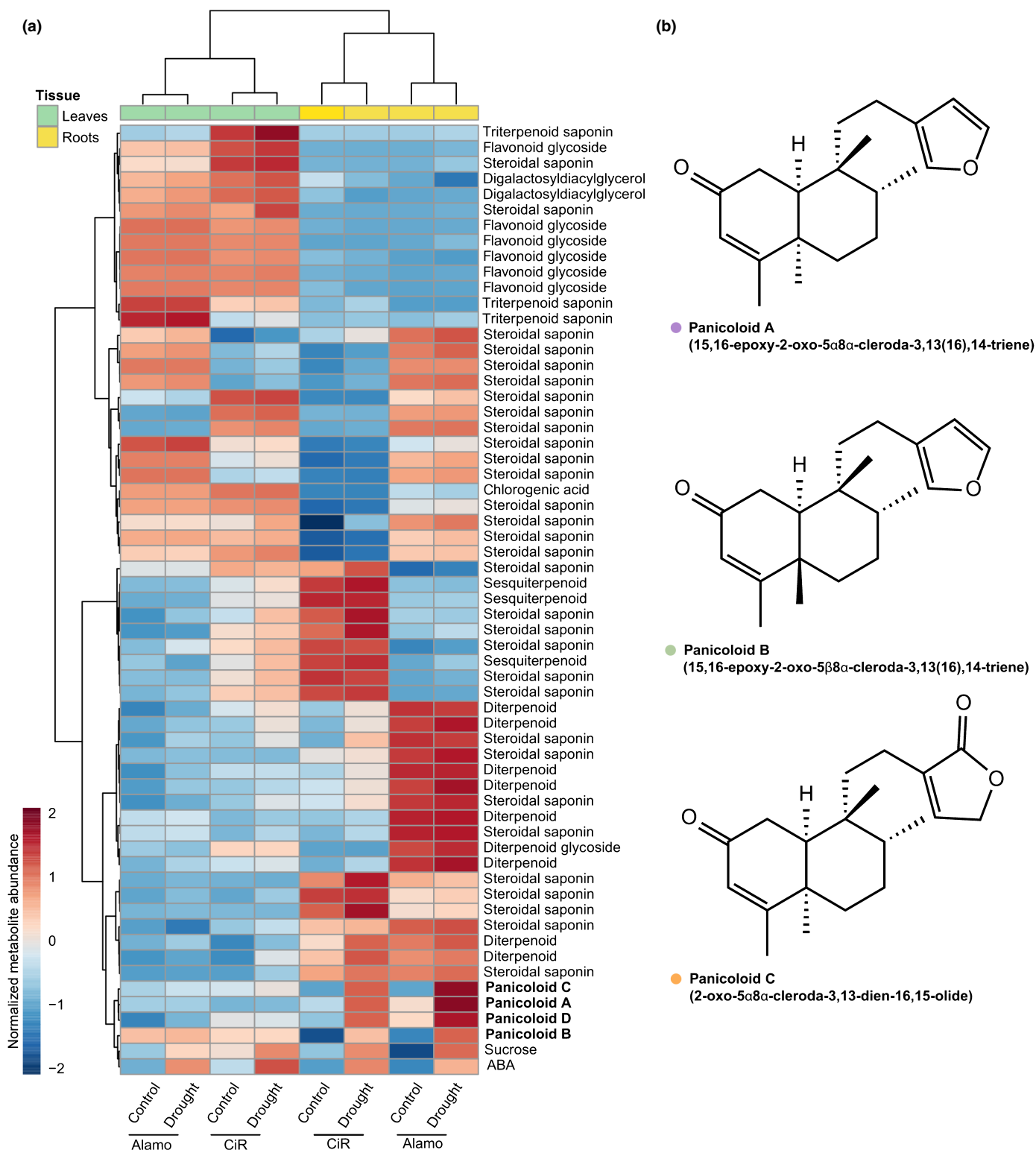
Fig. 8 (a) Hierarchical cluster analysis of select specialized metabolite accumulation patterns in switchgrass (*Panicum virgatum*). Sucrose and abscisic acid (ABA) abundance provide as drought-related reference metabolites. Metabolite annotations are based on matching *m/z* ratios, retention time and fragmentation patterns against online databases. (b) Structures of drought-induced diterpenoids, 15,16-epoxy-2-oxo-5α8α-cleroda-3,13(16),14-triene (*m/z* 301, panicoloid A), 15,16-epoxy-2-oxo-5β8α-cleroda-3,13(16),14-triene (*m/z* 301, panicoloid B) and 2-oxo-5α8α-cleroda-3,13-dien-16,15-olide (*m/z* 317, panicoloid C), isolated from drought-stressed switchgrass roots. Metabolite abundance is based on five biological replicates.

like genes in both Alamo and Cave-in-Rock is consistent with an increase in ABA observed in both genotypes and tissues in response to drought stress. While prior studies that showed increased ABA and sugar accumulation in drought-tolerant switchgrass genotypes (Liu *et al.*, 2015), the final concentration of ABA in drought stressed plants was at comparable levels in both genotypes in our study, whereas the concentration in the control plants was lower in Alamo, resulting in a higher fold-change/increase in Alamo when compared to Cave-in-Rock. Notably, the specific genes of the earlier gene families being differentially expressed differed between Alamo and Cave-in-Rock, suggesting that switchgrass genotypes recruit specific genes governing stress response mechanisms.

Pathways of general and specialized metabolism showed overall comparatively moderate differential gene expression in response to drought stress with apparent metabolic differences between leaf and root tissue. Accumulation of sucrose and ABA in Alamo and Cave-in-Rock tissues is consistent with previously demonstrated switchgrass drought responses (Liu *et al.*, 2015). In addition, the observed major contribution of phospholipids to metabolic alterations in leaves of both genotypes may be related to an upregulation of pathways involved in membrane lipid systems and cell wall biosynthesis as shown in, for example, drought-resistant maize lines (Zhang *et al.*, 2020). Additional phospholipid roles in drought tolerance may include maintenance of membrane integrity or mitigation of drought-related cell damage (Hamrouni *et al.*, 2001), as well as signaling processes during water deficiency as reported in selected drought-resistant species (Quartacci *et al.*, 1995; Moradi *et al.*, 2017). Contrasting drought-related flavonoid functions in, for example, wheat (*Triticum aestivum*) and other species (Ma *et al.*, 2014; Gai *et al.*, 2020), leaf flavonoid glycosides did not accumulate in response to drought in either switchgrass genotype, despite a moderate upregulation of select pathway genes such as *CHS* in drought-stressed plants. Similarly, steroidal and triterpenoid saponins were identified in switchgrass leaves, and have been shown to increase as part of the leaf cuticular waxes in response to drought (Kim *et al.*, 2007). However, our metabolite analysis did not show significant drought-elicited triterpenoid accumulation that would support a similar function in switchgrass.

Different from leaves, steroidal and other triterpenoid saponins as well as diterpenoids constituted the major determinants of metabolic differences in drought-stressed roots. Notably, MEP and MVA pathway genes showed no or very minor patterns of drought-inducible expression in Alamo or Cave-in-Rock, indicating that no major change in the production of terpenoid precursors occurs in response to drought. One exception is the putative *GGPPS*, *Pavir.6NG089000*, that is expressed in Alamo but not Cave-in-Rock roots and may contribute to differences in terpenoid metabolism between these genotypes. This apparent lack of drought activation of terpenoid backbone pathways suggests that terpenoid accumulation has to derive from existing precursor pools via changes in pathway branches *en route* to specific terpenoids. Indeed, in leaves and roots of Alamo, but not Cave-in-Rock, downstream triterpenoid-metabolic pathway genes increased under drought conditions. Interestingly, no apparent

triterpenoid-biosynthetic gene clusters were identified in the switchgrass genome, which differentiates switchgrass from other plant species where triterpenoid metabolism is commonly arranged in form of often stress-inducible biosynthetic clusters (Liu *et al.*, 2020; Bai *et al.*, 2021). Despite the lack of apparent genomic clusters, clear co-expression patterns were observed for several *TTS* genes as well as *sterol 3-β-glucosyltransferases* and *P450* genes of the *CYP71A*, *CYP94D* and *CYP90B* families, thus supporting the presence of co-expressed pathways toward specific triterpenoids. The identification of diverse mixtures of diosgenin and closely related triterpenoid saponins in roots of several upland and lowland ecotypes, including Alamo and Cave-in-Rock, supports this hypothesis (Lee *et al.*, 2009; Li *et al.*, 2022). However, the annotated triterpenoid metabolites were not significantly enriched in response to drought in either genotype, suggesting that the inducible expression of triterpenoid pathways in Alamo is related to distinct drought-stress responses. It can be speculated that root triterpenoids serve antioxidant functions to mitigate oxidative damage caused by water deficiency as shown in Arabidopsis and other species (Posé *et al.*, 2009; Nasrollahi *et al.*, 2014; Puente-Garza *et al.*, 2017). Also, recent studies have demonstrated bioactive triterpenoids in roots exudates of soybean (*Glycine max*) and tomato (*Solanum lycopersicum*) that aid the assembly of the root microbiome to confer robustness against environmental stresses (Fujimatsu *et al.*, 2020; Nakayasu *et al.*, 2021). While distinct microbiome responses to drought stress have been reported in upland and lowland switchgrass ecotypes (Liu *et al.*, 2021), the role of specialized metabolites such as saponins in these interactions is yet to be discovered.

Unlike root triterpenoids, significant drought-induced accumulation of several diterpenoids in roots supports a role in drought response mechanisms. Although requiring further biological studies, the higher abundance of these diterpenoids in Alamo as compared to Cave-in-Rock may contribute to the distinct stress resilience in these genotypes. In addition, accumulation in both Alamo and Cave-in-Rock support a role of these metabolites in drought responses rather than general stress responses associated with the more pronounced wilting phenotype observed in Cave-in-Rock. Structural analysis identified three compounds as oxygenated clerodane furanoditerpenoids, named here panicoloid A–C, which likely represent derivatives of furanoditerpenoid scaffolds recently identified in switchgrass (Pelot *et al.*, 2018; Muchlinski *et al.*, 2021). Notably, the enantiomeric stereochemistry of panicoloid B and panicoloid C is likely derived from the activity of yet unidentified diTPS functionally related to the CLPP synthase PvCPS1. Drought-induced gene expression increases of characterized pathway genes toward clerodane-type furanoditerpenoids, including the diTPS *PvCPS1* and the P450 genes *CYP71Z25*, *CYP71Z26* and *CYP71Z28* supports a role of these pathway genes in panicoloid biosynthesis. Additional co-expression of select P450s of the CYP99 family and predicted short-chain alcohol dehydrogenases/reductases, shown to function in specialized diterpenoid metabolism in maize and rice (Swaminathan *et al.*, 2009), suggests possible functions in the position-specific oxygenation reactions toward panicoloid biosynthesis. Similar to triterpenoid metabolism, the

lack of co-expression of these genes in the drought-susceptible Cave-in-Rock genotype may support a role of panicoloids in switchgrass drought responses. Combined with the abundance of yet unidentified diterpenoids in switchgrass roots, drought-elicited co-expression patterns of additional predicted *syn-CPP synthase* genes (*PvCPS9*, *PvCPS10*) and characterized class I diTPS forming *syn*-pimarane diterpenoids (*PvKSL4*, *PvKSL5*) suggest the presence of a broader diversity of drought-induced diterpenoids in switchgrass. Similar clerodane-type furanoditerpenoids have also been identified in species of *Vellozia spec.* (Pinto *et al.*, 1994), *Solidago spec.* (Anthonsen *et al.*, 1973; McCrindle *et al.*, 1976), and *Croton campestris* (El Babili *et al.*, 1998), where they will have evolved independently given the phylogenetic distance between these plant genera. While the drought-induced expression of diterpenoid-metabolic genes and associated accumulation of panicoloids and possibly other diterpenoids supports a role in switchgrass drought tolerance, the underlying mechanisms will require future investigation. However, drought-related diterpenoid bioactivities have recently been supported in other monocots. For example, maize studies demonstrated the accumulation of specialized kauralexin and dolabralexin diterpenoids in response to oxidative, drought and salinity stress (Christensen *et al.*, 2018; Mafu *et al.*, 2018), and diterpenoid-deficient maize mutants show decreased resilience to abiotic stress (Vaughan *et al.*, 2015). Additionally, antioxidative functions in relation to drought stress have been shown for select diterpenoids (Munné-Bosch & Alegre, 2003), and diterpenoid roles in the root microbiome assembly have been suggested based on changes in the microbiome composition in the kauralexin- and dolabralexin-deficient maize *an2* mutant (Murphy *et al.*, 2021).

Collectively, these findings exemplify the power of combining transcriptomic and in-depth metabolite analyses to accelerate the discovery of plant specialized pathways and products and enable a deeper investigation of their relevance and role in plant stress responses. This approach revealed common and distinct drought-induced metabolic changes in switchgrass genotypes of contrasting drought tolerance. These insights provide the foundation for future targeted genetic studies to investigate the diversity and protective function of terpenoids and other specialized metabolites in switchgrass drought tolerance.

Acknowledgements

Competing interests

None declared.

Author contributions

PZ, KT and RLL conceived the original research and oversaw data analysis; KT conducted plant drought stress experiments and transcriptome analysis; XL and KT performed metabolite profiling and analysis; ATM, PY, and DJT performed NMR structural analyses; DD and YC assisted with plant harvesting, sampling, and sample processing; KT and PZ wrote the original article draft with editing by all authors. All authors have read and approved the manuscript.

ORCID

Danielle Davisson https://orcid.org/0000-0001-5570-0301
Robert L. Last https://orcid.org/0000-0001-6974-9587
Xingxing Li https://orcid.org/0000-0002-7725-0329
Amy T. Merrill https://orcid.org/0000-0003-4801-1721
Dean J. Tantillo https://orcid.org/0000-0002-2992-8844
Kira Tiedge https://orcid.org/0000-0002-7239-6767
Ping Yu https://orcid.org/0000-0001-7610-6512
Philipp Zerbe https://orcid.org/0000-0001-5163-9523

Data availability

The RNA-sequencing data were submitted to the Sequence Read Archive (SRA), accession no. PRJNA644234.

References

Anthonsen T, Henderson M, Martin A, Murray R, McCrindle R, McMaster D. 1973. Constituents of Solidago species. Part IV. Solidagoic acids A and B, diterpenoids from *Solidago gigantea* var. *serotina*. *Canadian Journal of Chemistry* 51: 1332–1345.

Ayyappan V, Saha MC, Thimmapuram J, Sripathi VR, Bhide KP, Fiedler E, Hayford RK, Kalavacharla V. 2017. Comparative transcriptome profiling of upland (VS16) and lowland (AP13) ecotypes of switchgrass. *Plant Cell Reports* 36: 129–150.

Bai Y, Fernández-Calvo P, Ritter A, Huang AC, Morales-Herrera S, Bicalho KU, Karady M, Pauwels L, Buyst D, Njo M *et al.* 2021. Modulation of *Arabidopsis* root growth by specialized triterpenes. *New Phytologist* 230: 228–243.

Casler MD, Tobias CM, Kaeppler SM, Buell CR, Wang Z-Y, Cao P, Schmutz J, Ronald P. 2011. The switchgrass genome: tools and strategies. *The Plant Genome Journal* 4: 273–282.

Challinor AJ, Watson J, Lobell DB, Howden SM, Smith DR, Chhetri N. 2014. A meta-analysis of crop yield under climate change and adaptation. *Nature Climate Change* 4: 287–291.

Christensen SA, Huffaker A, Sims J, Hunter CT, Block A, Vaughan MM, Willett D, Romero M, Mylroie JE, Williams WP *et al.* 2018. Fungal and

herbivore elicitation of the novel maize sesquiterpenoid, zealexin A4, is attenuated by elevated CO$_2$. *Planta* 247: 863–873.

Ciura J, Szeliga M, Grzesik M, Tyrka M. 2017. Next-generation sequencing of representative difference analysis products for identification of genes involved in diosgenin biosynthesis in fenugreek (*Trigonella foenum-graecum*). *Planta* 245: 977–991.

Ding Y, Northen TR, Khalil A, Huffaker A, Schmelz EA. 2021. Getting back to the grass roots: harnessing specialized metabolites for improved crop stress resilience. *Current Opinion in Biotechnology* 70: 174–186.

Dührkop K, Nothias L-F, Fleischauer M, Reher R, Ludwig M, Hoffmann MA, Petras D, Gerwick WH, Rousu J, Dorrestein PC *et al.* 2021. Systematic classification of unknown metabolites using high-resolution fragmentation mass spectra. *Nature Biotechnology* 39: 462–471.

El Babili F, Moulis C, Bon M, Respaud M-J, Fourasté I. 1998. Three furano-diterpenes from the bark of *Croton campestris*. *Phytochemistry* 48: 165–169.

Fujimatsu T, Endo K, Yazaki K, Sugiyama A. 2020. Secretion dynamics of soyasaponins in soybean roots and effects to modify the bacterial composition. *Plant Direct* 4: e00259.

Gai Z, Wang Y, Ding Y, Qian W, Qiu C, Xie H, Sun L, Jiang Z, Ma Q, Wang L *et al.* 2020. Exogenous abscisic acid induces the lipid and flavonoid metabolism of tea plants under drought stress. *Scientific Reports* 10: 12275.

Hamrouni I, Salah HB, Marzouk B. 2001. Effects of water-deficit on lipids of safflower aerial parts. *Phytochemistry* 58: 277–280.

Horie K, Inoue Y, Sakai M, Yao Q, Tanimoto Y, Koga J, Toshima H, Hasegawa M. 2015. Identification of UV-induced diterpenes including a new diterpene phytoalexin, phytocassane F, from rice leaves by complementary GC/MS and LC/MS approaches. *Journal of Agricultural and Food Chemistry* 63: 4050–4059.

Kim D, Paggi JM, Park C, Bennett C, Salzberg SL. 2019. Graph-based genome alignment and genotyping with HISAT2 and HISAT-genotype. *Nature Biotechnology* 37: 907–915.

Kim KS, Park SH, Kim DK, Jenks MA. 2007. Influence of water deficit on leaf cuticular waxes of soybean (*Glycine max* [L.] Merr.). *International Journal of Plant Sciences* 168: 307–316.

Kim W, Iizumi T, Nishimori M. 2019. Global patterns of crop production losses associated with droughts from 1983 to 2009. *Journal of Applied Meteorology and Climatology* 58: 1233–1244.

Lee ST, Mitchell RB, Wang Z, Heiss C, Gardner DR, Azadi P. 2009. Isolation, characterization, and quantification of steroidal saponins in switchgrass (*Panicum virgatum* L.). *Journal of Agricultural and Food Chemistry* 57: 2599–2604.

Li X, Sarma SJ, Sumner LW, Jones AD, Last RL. 2022. Switchgrass metabolomics reveals striking genotypic and developmental differences in specialized metabolic phenotypes. *Journal of Agricultural and Food Chemistry* 70: 8010–8023.

Liu T-Y, Chen M-X, Zhang Y, Zhu F-Y, Liu Y-G, Tian Y, Fernie AR, Ye N, Zhang J. 2019. Comparative metabolite profiling of two switchgrass ecotypes reveals differences in drought stress responses and rhizosheath weight. *Planta* 250: 1355–1369.

Liu T-Y, Ye N, Wang X, Das D, Tan Y, You X, Long M, Hu T, Dai L, Zhang J *et al.* 2021. Drought stress and plant ecotype drive microbiome recruitment in switchgrass rhizosheath. *Journal of Integrative Plant Biology* 63: 1753–1774.

Liu Y, Zhang X, Tran H, Shan L, Kim J, Childs K, Ervin EH, Frazier T, Zhao B. 2015. Assessment of drought tolerance of 49 switchgrass (*Panicum virgatum*) genotypes using physiological and morphological parameters. *Biotechnology for Biofuels* 8: 152.

Liu Z, Cheema J, Vigouroux M, Hill L, Reed J, Paajanen P, Yant L, Osbourn A. 2020. Formation and diversification of a paradigm biosynthetic gene cluster in plants. *Nature Communications* 11: 5354.

Lovell JT, MacQueen AH, Mamidi S, Bonnette J, Jenkins J, Napier JD, Sreedasyam A, Healey A, Session A, Shu S *et al.* 2021. Genomic mechanisms of climate adaptation in polyploid bioenergy switchgrass. *Nature* 590: 438–444.

Lovell JT, Schwartz S, Lowry DB, Shakirov EV, Bonnette JE, Weng X, Wang M, Johnson J, Sreedasyam A, Plott C *et al.* 2016. Drought responsive gene expression regulatory divergence between upland and lowland ecotypes of a perennial C4 grass. *Genome Research* 26: 510–518.

Lowry DB, Behrman KD, Grabowski P, Morris GP, Kiniry JR, Juenger TE. 2014. Adaptations between ecotypes and along environmental gradients in *Panicum virgatum*. *The American Naturalist* 183: 682–692.

Ma D, Sun D, Wang C, Li Y, Guo T. 2014. Expression of flavonoid biosynthesis genes and accumulation of flavonoid in wheat leaves in response to drought stress. *Plant Physiology and Biochemistry* 80: 60–66.

Mafu S, Ding Y, Murphy KM, Yaacoobi O, Addison JB, Wang Q, Shen Z, Briggs SP, Bohlmann J, Castro-Falcon G *et al.* 2018. Discovery, biosynthesis and stress-related accumulation of dolabradiene-derived defenses in maize. *Plant Physiology* 176: 2677–2690.

Magwanga RO, Lu P, Kirungu JN, Lu H, Wang X, Cai X, Zhou Z, Zhang Z, Salih H, Wang K *et al.* 2018. Characterization of the late embryogenesis abundant (LEA) proteins family and their role in drought stress tolerance in upland cotton. *BMC Genetics* 19: 6.

McCrindle R, Nakamura E, Anderson AB. 1976. Constituents of Solidago species. Part VII. Constitution and stereochemistry of the cis-clerodanes from *Solidago arguta* Ait. and of related diterpenoids. *Journal of the Chemical Society, Perkin Transactions* 1: 1590–1597.

McLaughlin S, Bouton J, Bransby D, Conger B, Ocumpaugh W, Parrish D, Taliaferro C, Vogel K, Wullschleger S. 1999. Developing switchgrass as a bioenergy crop. *Perspectives on New Crops and New Uses* 56: 282–299.

Meyer E, Aspinwall MJ, Lowry DB, Palacio-Mejía JD, Logan TL, Fay PA, Juenger TE. 2014. Integrating transcriptional, metabolomic, and physiological responses to drought stress and recovery in switchgrass (*Panicum virgatum* L.). *BMC Genomics* 15: 527.

Moradi P, Mahdavi A, Khoshkam M, Iriti M. 2017. Lipidomics unravels the role of leaf lipids in thyme plant response to drought stress. *International Journal of Molecular Sciences* 18: 2067.

Morrow WR, Gopal A, Fitts G, Lewis S, Dale L, Masanet E. 2014. Feedstock loss from drought is a major economic risk for biofuel producers. *Biomass and Bioenergy* 69: 135–143.

Muchlinski A, Chen X, Lovell JT, Köllner TG, Pelot KA, Zerbe P, Ruggiero M, Callaway Iii L, Laliberte S, Chen F. 2019. Biosynthesis and emission of stress-induced volatile terpenes in roots and leaves of switchgrass (*Panicum virgatum* L.). *Frontiers in Plant Science* 10: 1144.

Muchlinski A, Jia M, Tiedge K, Fell JS, Pelot KA, Chew L, Davisson D, Chen Y, Siegel J, Lovell JT *et al.* 2021. Cytochrome P450-catalyzed biosynthesis of furanoditerpenoids in the bioenergy crop switchgrass (*Panicum virgatum* L.). *The Plant Journal* 108: 1053–1068.

Munné-Bosch S, Alegre L. 2003. Drought-induced changes in the redox state of α-tocopherol, ascorbate, and the diterpene carnosic acid in chloroplasts of labiatae species differing in carnosic acid contents. *Plant Physiology* 131: 1816–1825.

Murphy KM, Edwards J, Louie KB, Bowen BP, Sundaresan V, Northen TR, Zerbe P. 2021. Bioactive diterpenoids impact the composition of the root-associated microbiome in maize (*Zea mays*). *Scientific Reports* 11: 333.

Murphy KM, Zerbe P. 2020. Specialized diterpenoid metabolism in monocot crops: biosynthesis and chemical diversity. *Phytochemistry* 172: 112289.

Nakayasu M, Ohno K, Takamatsu K, Aoki Y, Yamazaki S, Takase H, Shoji T, Yazaki K, Sugiyama A. 2021. Tomato roots secrete tomatine to modulate the bacterial assemblage of the rhizosphere. *Plant Physiology* 186: 270–284.

Nasrollahi V, Mirzaie-asl A, Piri K, Nazeri S, Mehrabi R. 2014. The effect of drought stress on the expression of key genes involved in the biosynthesis of triterpenoid saponins in liquorice (*Glycyrrhiza glabra*). *Phytochemistry* 103: 32–37.

Newbery F, Qi A, Fitt BD. 2016. Modelling impacts of climate change on arable crop diseases: progress, challenges and applications. *Current Opinion in Plant Biology* 32: 101–109.

Olvera-Carrillo Y, Campos F, Reyes JL, Garciarrubio A, Covarrubias AA. 2010. Functional analysis of the group 4 late embryogenesis abundant proteins reveals their relevance in the adaptive response during water deficit in *Arabidopsis*. *Plant Physiology* 154: 373–390.

Pang Z, Chong J, Zhou G, de Lima Morais DA, Chang L, Barrette M, Gauthier C, Jacques P-É, Li S, Xia J. 2021. METABOANALYST 5.0: narrowing the gap between raw spectra and functional insights. *Nucleic Acids Research* 49: W388–W396.

Park HL, Lee SW, Jung KH, Hahn TR, Cho MH. 2013. Transcriptomic analysis of UV-treated rice leaves reveals UV-induced phytoalexin biosynthetic pathways and their regulatory networks in rice. *Phytochemistry* **96**: 57–71.

Pelot KA, Chen R, Hagelthorn DM, Young CA, Addison JB, Muchlinski A, Tholl D, Zerbe P. 2018. Functional diversity of diterpene synthases in the biofuel crop switchgrass. *Plant Physiology* **178**: 54–71.

Pinto AC, Garcez WS, Queiroz PP, Fiorani NG. 1994. Clerodanes and tetranorclerodane from *Vellozia bicolor*. *Phytochemistry* **37**: 1115–1117.

Pokhrel Y, Felfelani F, Satoh Y, Boulange J, Burek P, Gädeke A, Gerten D, Gosling SN, Grillakis M, Gudmundsson L *et al.* 2021. Global terrestrial water storage and drought severity under climate change. *Nature Climate Change* **11**: 226–233.

Posé D, Castanedo I, Borsani O, Nieto B, Rosado A, Taconnat L, Ferrer A, Dolan L, Valpuesta V, Botella MA. 2009. Identification of the Arabidopsis dry2/sqe1-5 mutant reveals a central role for sterols in drought tolerance and regulation of reactive oxygen species. *The Plant Journal* **59**: 63–76.

Puente-Garza CA, Meza-Miranda C, Ochoa-Martínez D, García-Lara S. 2017. Effect of *in vitro* drought stress on phenolic acids, flavonols, saponins, and antioxidant activity in *Agave salmiana*. *Plant Physiology and Biochemistry* **115**: 400–407.

Quartacci MF, Pinzino C, Sgherri CL, Navari-Izzo F. 1995. Lipid composition and protein dynamics in thylakoids of two wheat cultivars differently sensitive to drought. *Plant Physiology* **108**: 191–197.

Savary S, Willocquet L, Pethybridge SJ, Esker P, McRoberts N, Nelson A. 2019. The global burden of pathogens and pests on major food crops. *Nature Ecology & Evolution* **3**: 430–439.

Schmelz EA, Huffaker A, Sims JW, Christensen SA, Lu X, Okada K, Peters RJ. 2014. Biosynthesis, elicitation and roles of monocot terpenoid phytoalexins. *The Plant Journal* **79**: 659–678.

Sumner LW, Amberg A, Barrett D, Beale MH, Beger R, Daykin CA, Fan TW, Fiehn O, Goodacre R, Griffin JL *et al.* 2007. Proposed minimum reporting standards for chemical analysis Chemical Analysis Working Group (CAWG) Metabolomics Standards Initiative (MSI). *Metabolomics* **3**: 211–221.

Swaminathan S, Morrone D, Wang Q, Fulton DB, Peters RJ. 2009. CYP76M7 Is an *ent*-Cassadiene C11α-hydroxylase defining a second multifunctional diterpenoid biosynthetic gene cluster in rice. *Plant Cell* **21**: 3315–3325.

Tiedge K, Muchlinski A, Zerbe P. 2020. Genomics-enabled analysis of specialized metabolism in bioenergy crops: current progress and challenges. *Synthetic Biology* **5**: ysaa005.

USDA Farm Service Agency. 2021. *Secretarial drought designations for 2021*. [WWW document] URL https://www.fsa.usda.gov/Assets/USDA-FSA-Public/usdafiles/Disaster-Assist/Secretarials/2021-Secretarial-Disasters/ALL_Drought_CY2021.pdf [accessed 10 March 2022].

Vaughan MM, Christensen S, Schmelz EA, Huffaker A, McAuslane HJ, Alborn HT, Romero M, Allen LH, Teal PE. 2015. Accumulation of terpenoid phytoalexins in maize roots is associated with drought tolerance. *Plant, Cell & Environment* **38**: 2195–2207.

Yao L, Cheng X, Gu Z, Huang W, Li S, Wang L, Wang YF, Xu P, Ma H, Ge X. 2018. The AWPM-19 family protein OsPM1 mediates abscisic acid influx and drought response in rice. *Plant Cell* **30**: 1258–1276.

Zhang Q, Liu H, Wu X, Wang W. 2020. Identification of drought tolerant mechanisms in a drought-tolerant maize mutant based on physiological, biochemical and transcriptomic analyses. *BMC Plant Biology* **20**: 315.

Supporting Information

Additional Supporting Information may be found online in the Supporting Information section at the end of the article.

Fig. S1 Available water content in the soil during the treatment.

Fig. S2 Differentially expressed genes between all groups after 4 wk of drought treatment.

Fig. S3 Identification of significantly enriched metabolic pathways at the end of the treatment via Gene Ontology term analysis.

Fig. S4 Liquid chromatography–mass spectrometry chromatograms and spectra of identified panicoloids.

Fig. S5 Diterpenoid network in switchgrass.

Fig. S6 Nuclear magnetic resonance analysis of panicoloids A–C.

Table S1 Complete list of differentially expressed genes.

Table S2 Permutational multivariate analysis of variance of gene expression levels and metabolite abundances.

Table S3 Enrichment of Gene Ontology terms and Kyoto Encyclopedia of Genes and Genomes pathways in Alamo and Cave-in-Rock.

Table S4 Complete list of the calculated FPKM (fragments per kilobase of transcript per million mapped reads) values for all genes.

Table S5 List of all mass features from the positive mode liquid chromatography–mass spectrometry dataset that were selected for the downstream statistical analysis.

Table S6 Statistical analysis for detected liquid chromatography–mass spectrometry features of annotated specialized metabolites.

Please note: Wiley Blackwell are not responsible for the content or functionality of any Supporting Information supplied by the authors. Any queries (other than missing material) should be directed to the *New Phytologist* Central Office.